Integrated Techniques To Identify Consequences Of Sinkhole Hazards For Constructing Housing Complexes On Carbonate Karst Terrains In Perak, Peninsular Malaysia

Riyadh R. Yassin, Ros Fatihah Muhammad, Samsudin Hj Taib

Department of Geology, Faculty of Science, University of Malaya, 50603 Kuala Lumpur, Malaysia.

Research Highlights:

Integrated techniques were performed across two housing complex construction sites north Ipoh city, Perak state, peninsular Malaysia.

An assessment of the situation was surmised from the subsurface images. Subsequently an estimation of the possibility of a collapse occurring due to sinkhole was prepared.

Interpretation of geophysical data indicated that both low resistivity and high conductivity anomalies extend along the proposed area in both construction sites.

Early planning is needed to minimize the risk to structures in construction sites over karstified carbonate bedrock.

Initial consolidation of geo grading technique, driven piles to rock head pinnacles and control the drainage works must be put into operation in these sites.

Abstract

Engineers are exposed to numerous problems while designing structures that would be overlying carbonate karst terrain which are characterized by various bedrock solution features such as caves, sinkholes, depressions, enlarged joints and fractures, and internal drainages that can exert a negative impact on the use of land for construction projects and can directly have an effect on the construction structures that are to be founded in carbonate karst terrains. Furthermore can indirectly have a consequence in the future, many years after the completion of the construction project. In spite of subsidence damage resulting from carbonate dissolution causing massive losses all over the world, the causes are well addressed in few areas only. The integrated of geological, geophysical, aerial photographs and satellite images will be represented in this paper through identification techniques. In this study a Two-dimensional electrical resistivity tomography (ERT) survey was performed across two housing complex construction sites north Ipoh city, Perak state, peninsular Malaysia to image the subsurface and locate evidence for near surface karstic features such as voids or cavities including sinkholes and to estimate the depth of the bedrock. Furthermore to estimate whether geophysical technique can identify such features or not. Six resistivity traverses or profiles were conducted

along the survey area at each of the two construction sites. The orientation, extension and the degree of inclination of those profiles are shown in the location map. The correct resistivity data was interpreted using res2dinv software. An assessment of the situation was surmised from the subsurface images. Subsequently an estimation of the possibility of a crumple occurring due to these cavities or voids was prepared. This study also displayed that high resolution Electrical Resistivity Tomography (ERT) can be effectively implemented to reflect the bedrocks. It's also completely suitable for differentiating surficial soil, clay, weathered rocks, compact or intact rocks and air-filled karstic voids or cavities and intensely fractured rocks. These features have an effect on many construction site locations in areas extended over carbonate rocks, causing disturbance in construction works which can supply to the maximization of the overall cost. Interpretation of geophysical data indicated that both low resistivity and high conductivity anomalies extend along the proposed area in both construction sites. The ambiguities anomaly observed in construction site # 1 indicate the area has been exaggerated by a sinkhole that thus contains clay and water, making the area less resistive to electrical current. The ambiguities anomaly observed in construction site #2 indicate the area has been affected by several sinkholes and tubular anomalies that contain both clay and sandy clay. The appearance of many high-flying sinkholes in the affected segment is mostly attributed to karstic activity. In accordance with to the characteristics of morphological features of karstic ground conditions by (A. C. Waltham and P. G. Fookes, 2005), the karst in construction site site#1 found between profile 1 and profile 6 is an older or complex karst KIV. The karst in construction site#2 found between profile 1 and profile 3 is a youthful karst KII. Afterwards the karst type changed over profile#5 to profile #6 to mature karst KIII.

Early planning is needed to mitigate or minimize the risk of structures in these construction sites over karstified carbonate bedrock. Initial consolidation of geo grading technique, driven piles to rock head pinnacles and control drainage works must be put into operation in these sites.

Keywords: Integrated Techniques; Identify consequences; Sinkhole Hazards; carbonate karst terrains; Constructing Housing Complexes; Perak - peninsular Malaysia.

Introduction

In that case the position and condition of carbonate bedrocks such as limestone, dolomite, dolomitic limestone or marbleized limestone and its appearance is important for engineering constructions such as buildings, housing complexes and roads projects.

Sinkholes can concern construction sites which overlie carbonate rocks causing construction delays, stability problems, which may amplify the increase in cost due to cracking of walls, building foundation collapse, road with pavement subsidence

and cracking. These are only some examples of the problems associated with sinkhole, karstic cavity and voids. Structural instability associated with these features can arise as a result of sudden collapse of the ground surface or as a less catastrophic but recurring drainage problem. Within karst regions, design and execution will be expensive regarding present and future structures. Besides, borings drilled within karsts regions do not overlap areas of concern in the subsurface. Inappropriate and mismanaged borings cannot provide ample subsurface data for analysis and at the same time can also misrepresent the subsurface system which may lead additional cost for corrective design or additional analysis. Rapid reconnaissance surveys using satellite images and surface geophysical techniques incorporated with a boring plan are the best obtainable options that can be used to aid in the suitable location of test borings to identify or distinguish the subsurface features related to karst development.

The 2D resistivity imaging technique was preferred for the subsurface investigations instead of other geophysical methods for the high contrast or disparity in resistivity values between different types of sediments like carbonate rock and clay or soil, air or water in-filled cavity or voids compared to the bordering or surrounding limestone bedrock. These entire elements reflector reproduce the use of resistivity imaging method to outline and delineate the boundary between bedrock and overburden. Apart from that, this method is not unmanageable in respect of time for small scale projects in both pre ability and post ability processing steps, making it most appropriate for investigations.

Electrical resistivity tomography surveys were functional at two constructions sites to the north of Ipoh city. Construction site #1 is located at Klebang Putra – Klebang Green and Construction site #2 is located at Medan Klebang Restu-Klebang Damai, north Ipoh city, Perak state, Malaysia peninsular. The locations of the construction sites were shown in Figure 1.

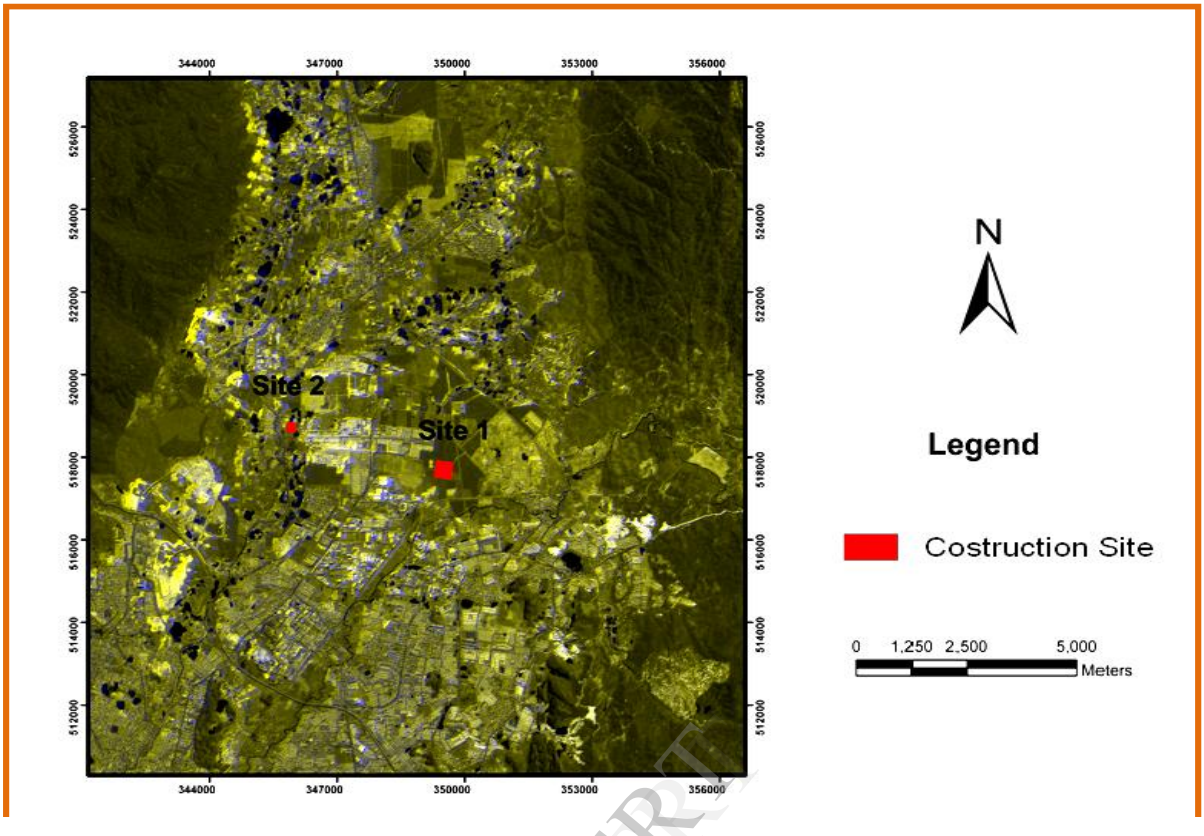

Figure 1: Satellite Image (2008) viewing the location of construction sites #1and site #2 north of Ipoh city (Kinta valley)

The objective of this survey is to:

Imaging the subsurface carbonate karst bed rocks to locate evidence for near surface karstic features such as voids, cavities, channels, pipes and sinkholes.
Figure out whether clay or air-filled karstic voids or cavities are present in the subsurface.
Estimate depth of the marbleized limestone bedrock.
Estimate the, depth, shape , type and understand the origin of the karst features such as sinkhole.

Producing the geological model clarified the study area from the geophysical data.
Evaluate the subsurface karst ground conditions which based on features that occurring in the intact carbonate rocks and its level and describe if that can result in potentially dangerous collapse or ground failures at construction sites which superimpose these features.
Identify subsurface conditions that might collaborating the reliability of any proposed future work in these sites, for example, an inactive sinkhole in-filled with thick clay. Under-compacted clay could represent a critical problem because the

clays could be accumulated under load resulting in the leakage down to the bed rock.

Geology of study area

Topography and geomorphology of study area

Kinta Valley is a triangular-shaped or V - shaped valley bounded by the Main Range on the east which rise to 867 m above mean sea level and Kledang Range in the west. The northern tip of the triangle starts at around Chemore town in the north. The valley in this region broaden to about 7 km and broaden in the south around Kampar town to reach in this region about 20 km . This valley extended over a distance of about 45 km from north to south. The first tower karst observed in Kinta valley is Gunung Kanthan in the north and the last is Gunung Tempurung in the south. The alluvial plain is situated at about 60 m to 80 m above mean sea level. This is an area that has been under active tin-mining and most of the tower karst and subsurface karst are exposed here in this valley.

Major rivers originating from the granitic Main Range highland drains most of the karstic land in the study area. The famous one drained Kinta Valley is Sungai Kinta extended from the northeast down to Bota in the southwest to meet the Sungai Perak. Major tributaries of Sungai Perak drain into the valley and run through the limestone towers from the east and northeast of the valley are Sungai Pinji, Sungai Raia, Sungai Dipang, Sungai Kinta, Sungai Tempurung and Sungai Kampar. Those tributaries bringing the alluvial deposits over the eroded marbleized limestone and creating a flood plain across the low lying valley.

Lithology of study area

In Kinta valley the lithology of the study area are made up of four main types, each producing a different landscape. They are:

Carbonate rocks forming Kinta Limestone in which has been going through tropical karstification to form steep sided tower and cockpit towers protruding across the enormous plain.

Granite bodies of the Main Range and Kledang Range (series) that flank the plain in the east and west respectively forming rugged ranges of up to 1000 m above mean sea level.

Schist which makes up the rolling landscape of the valley.

Quaternary alluvial deposits that has been deposited across the valley and form an enormous plain.

Limestone of Kinta valley

Kinta Valley lies to the west of the Main Granitic Range and east of the Kledang Granitic Range. Geologically, the Kinta Valley is underlain by Kinta Limestone of Silurian to Permian age are confined to the central axis of the valley. It's including several relatively thin argillaceous beds, and exceeds 3000 m in stratigraphic thickness (Ingham and Bradford, 1960; Suntharalingam, 1968). They were folded and recrystallized by regional

metamorphism in the Late Triassic. The Main Range which averages about 1000 m above mean sea level is made up mostly of coarse-grained porphyritic biotite granite. A number of geologists had described the formation of the Kinta Valley to block faulting occurring at the contacts between the granites and the meta-sedimentary rocks (Gobbett, 1973). Carbonate rocks forming karst in these parts of Kinta Valley are mostly marbleized and dolomitized of Upper Palaeozoic age. Calcitic marble is dominant although patches of dolomite are found in some parts such as Simpang Pulai area and Kampar. Gua Tempurung is 90% calcitic and shows clear differences in size from coarser in the eastern part of the hill to finer to the west due to the close metamorphic contact with the granite to its east (Rashidah, 1998).

Only 30% of limestone in Kinta Valley occurs as limestone hills while the rest are subsurface karst (Muhammad, 2003). Rivers from the two highlands provide uninterrupted supply of allogenic water to the foot plain and consequently create wet and swampy conditions. Studies using Micro Erosion Meter gives the assessment of limestone deprivation rates for standing water, running and under sub-aerial condition and the values are 224 mm/ka, 369 mm/ka and 134 mm/ka (Muhammad, 2002) correspondingly.

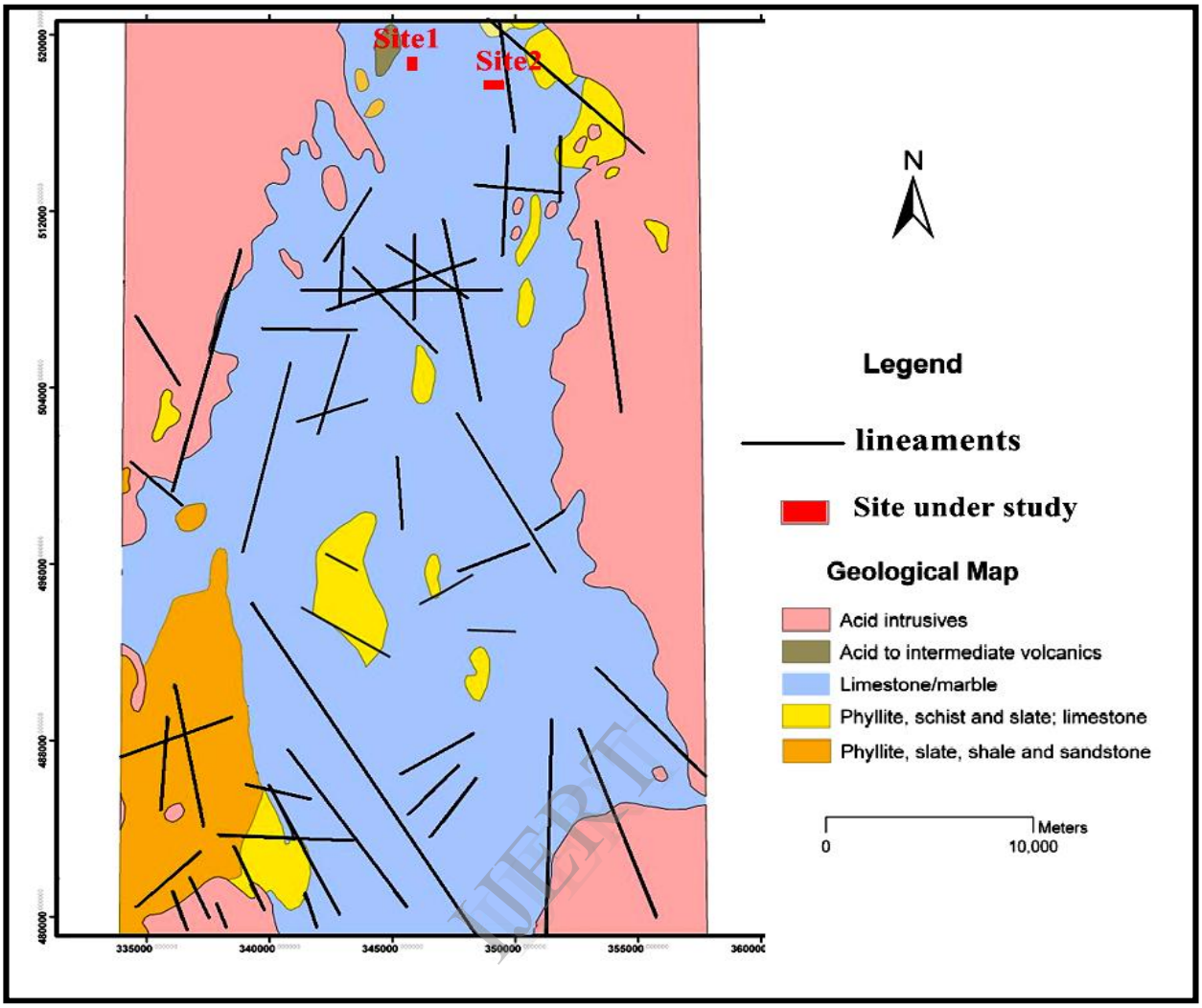

Figure 2: Geological map of Perak state including the location of construction sites #1and #2 north of Ipoh city, (Kinta valley)

Development of the karst phenomena in sungai Perak basin (Kinta valley)

The important elements which play major roles in determining and development of the karst formation in the Sungai Perak Basin are due to a number of elements that were working together in the geologic past. The karst in the Sungai Perak Basin has developed under these conditions:

Tectonic condition through the past period.

Varying of climate conditions through the past period from humid tropical to seasonal savanna and arid seasonal.

Constant supplying of water from rainfall in most seasons.

The conditions of flood plain in Kinta valley form an area of active fluvial activities with availability of large amounts of allogenic water passing through the limestone karst.

several geologists have suggested that major karstification is controlled by the structures in the areas when it's occurred. The structural Geology in the limestone of

Kinta valley area are dominated by faults and folds oriented north-south which gives a noticeable grains to the landscape especially to the orientation of (mogotes) isolated, steep-sided, residual, hills, which are composed of either limestone, marble, or dolomite and surrounded by nearly flat alluvial plains in the central part of the valley. Vertical and sub vertical joints and faults in the marble provide the main lines of weaknesses. The subsurface karst is characterized by the formation of rounded top pinnacles and irregularly-shaped sinkholes which had previously referred to as dolines. One of important aspect on the sub-surface karst in the study area particularly in Kinta valley is the presence of one or more concordant levels of the rounded top pinnacles that had been referred to as plat forming levels. It is believed that the sub-surface karst is developed below a cover of alluvial sediments during the geologic past (Yeap, 1998 and Dian, 1996). The opinions that at the early stage of pinnacle development due to the differential resistance of physical weathering of the rocks and the role of geological structures (bedding planes, joints, fault etc.) lead to the formation of pinnacles under cold climates of Tibet to developed.

Rainfall incorporated with dissolved carbon dioxide, which makes it a strong acid identified as carbonic acid (H_2CO_3). It will become more acidic as it filters through side soil, as there is more carbon dioxide in gaps in the soil – up to 100 times more than the atmosphere. The writer belief that the most imperative recent thought is the enhanced rainfall and elevated acidity of the rain in the last few decades of the 20^{th} and 21^{st} century in Malaysia and other countries in South East Asia are due to increase amount of liquefied carbon dioxide.

These are the consequence of volcanic and tectonic activity in the Pacific fire ring, with volcanoes in Indonesia and Philippines being the bordering and most active. A spectacular submarine volcanic eruption spews out huge columns of ash, smoke, gas and vapours thousands of feet into the Pacific Ocean sky. As well as land clearing activities by burning of large jungle areas in Indonesia results in the emission of large volumes of smoke into the air. Exhaust emissions from vehicles and waste emissions from factories significantly contribute to air pollution. All these events have a large impact on the development and quick dissolving process of carbonate rocks. The writer also belief that most of the biggest cave and channels in the limestone of Kenta valley due to reaction of sulfuric acid (H_2SO_4) with carbonate rocks can also be one of the corrosion factors in karst formation, this mechanism may also play a role, as O_2-rich surface waters seep into the ground, its brings oxygen which reacts with sulfide present with Cassiterite into the ground surface of Kinta valley area, the oxidation of sulfide leading to the formation of sulfuric acid. Sulfuric acid then reacts with calcium carbonate causing increased erosion within the limestone formation. The cover layers of alluvial deposits over marbleized limestone of Kenta valley contains soil-

piping or channels feature. The Tin (Cassiterite) was accumulated in this alluvial channels or pipes having been washed down from the granite ranges and carried by rivers as mentioned previously, which contain sulphur in its chemical deposits have a large impact on the development and quick dissolving process of carbonate rocks. Furthermore replacement deposits consist chiefly of Cassiterite and sulphide minerals deposits are found in replacement pipes in the Kinta Valley area. Those are replacing of dolomitic or calcareous sediments.

Engineering Classification of Karst Ground Condition

The dissolution of carbonate rocks such as limestone, dolomite and marbleized limestone by natural waters creates extensive karst landforms that can be very difficult ground for civil engineers. Karst features develops on soluble rocks, both at the surface and subsurface due to the rate of dissolution processes which depends on a number of factors, including power of rainfall, availability of surface water and its form of revive as well as groundwater, distribution of soil-cover, temperature and biological activity, the diffusion rate, autogenic content, structural weakness and lithology of the carbonate sub layers.

Sinkholes mostly were created on soluble carbonate rocks (limestone, dolomite, dolomitic limestone and marbleized limestone). Sinkholes developed at both the surface and subsurface due to the dissolution related with the difference in composition and associated processes and pose many problems, and are classified A. C. Waltham and P. G. Fookes, 2001, into six types, including the type subsidence sinkholes that formed in soil cover within karst terrains. Sinkholes have a wide-ranging destructive effect on many regions of the world. The creation of sinkholes may cause severe damage to man-made structures and may even menace human lives when they take place in a catastrophic way.

Voids in bedrock can hinder surface-water flow and disrupt the surface drainage system. Soil and other surface material may be washed into the underground network of cavities. Sometimes less tangible karsts can cause significant impact on water quality. Caves threaten foundation integrity when the width of the cave is greater than their roof thickness. The networks of consistent caves and voids allow contaminants such as sewage, landfill leachate, or hazardous chemicals to travel unimpeded into shallow aquifers that may supply drinking water. The issue of probable presence of solution features must be cautiously considered while making land-management decisions, including decisions for protecting water supply, locating septic systems and placing of waste disposal facilities. Rock head creating difficult ground to excavate and found with varies morphology from uniform to relief pinnacle.

An engineering classification of karst ground conditions was done by A.C. Waltham and P.G. Fookes, 2005, based on features that occur in the intact carbonate rock and characterizes the karst in terms of the complexity and difficulty to be encountered by the foundation engineer.

Identification of sinkholes and subsidence areas by applying geophysical technique

The assortment and application of geophysical techniques intended to reduce the sinkhole risk generally require the detection of the existing sinkholes and the explanation of the areas where unique sinkholes are most likely to occur in future. It is also significant to accumulate information of the size and frequency of the sinkhole events and the subsidence mechanisms and rates. However, it's usually a thorny task to identify the areas affected by carbonate dissolution subsidence. Sinkholes are usually enclosed by human activities, such as filling and development or natural attrition processes may eradicate them.

In general, sinkholes may have a very fine geomorphic appearance or the collapse produced by underground processes may be yet to reach the ground surface. It is required to examine as many sources of surface and subsurface information as possible to grant sufficient data about the past and existing subsidence movement in the study area. In order to partially rise above these difficulties, geophysical examination techniques can be used to detect the changes in the physical properties and the anomalies of the ground connected with air-filled, water-filled or sediment-filled cavities, breccias pipes, subsidence of structures ravel zones, synclinal hang down, down thrown blocks, irregularity of rock head topography and covered sinkholes. Major characteristics of the ambiguities must be acknowledged for some interfering methods such as excavating trenches, borehole drilling or applying of borehole probing.

There are extensive variety of a methods whose applicability and fitness depends largely on the investments available, type of necessary deposits, geological situation uncovered, the over covering or inter layers of the karsts, the topography of the area and the probable type of structures dissolution, the estimated type of structures subsidence, existence of interfere factors such as man-made services and the required penetration and declaration. Sinkhole activity has become obvious in developed areas through the deformation of roadway and building, intermittent services and other formation. Applying geophysical approaches for mapping the subsidence destruction, information on the spatial allocation of the subsidence can be gained and the major natural and human factors that control the dissolution and subsidence processes may also be conditional. Devastation of building can also be recorded on performance evidence

sheets to supply the data in a GIS and database system.

The best option is to apply two or more geophysical techniques and then evaluate the results with each other. It is wise to apply geophysical examination techniques on the sites prior to drilling as one of the phased sequences of investigation. The area with aberrations and the normal areas bereft of aberrations are recognized then delineated and planned for construction projects. Evaluation of the geophysical techniques used in karst areas have been presented by Hoover (2003) and Waltham et al. (2005). A number of previous geophysical studies in karst terrain as in applying (ERT) technique to map the bedrock surface, W. Zhou B.F. Beck J.B. Stephenson, 2000, a site in southern Indiana where limestone is covered by about 9 m of clayey soils. Forty-nine profiles were conducted over an area of approximately 42,037 m^2. The repeatability of ERT technique was evaluated by comparing the previous drilling section with interpreted ERT section from pairs of transects where they crossed each other. To identified the depth of mud-filled void and its extension, William E. Doll', Jonathan E. Nyquist, Philip J. Carpenter, Ronald D. Kaufmann, and Bradley J. Car-r', 2002, applied geophysical surveys at a site on the Oak Ridge Reservation (ORR), Tennessee, USA. The data suggest that an optimal scheme for detailed karst mapping might consist of multi electrode resistivity surveying followed by joint inversion of gravity and seismic Travel time data. The resistivity results could be used to produce an initial model for the seismic and gravity inversions. To identify buried sinkholes and other karst features in zone of karst terrain Kachentra neawsuparp and tanad soisa (2007) applied of 2D and 3D resistivity imaging resistivity (ERT) survey at Ban Pakjam in Huaiyod district, Trung province, in southern part of Thailand. The 2D resistivity surveys clearly show the central depression as well as resistivity contrasts between the cover sediments, delineating the in- filled sinkholes, underlying weathered bedrock and mapped the locations of sinkholes in this covered karst terrain.

Identifying Sinkholes by Employing of Aerial Photographs and Satellite images technique

Large-scale colour stereoscopic aerial photographs are very helpful for identifying sinkholes. The key limitation of aerial photographs and satellite images is that, depending on the scale and explanation of the images, it may not be feasible to pin down small or shallow sinkholes.

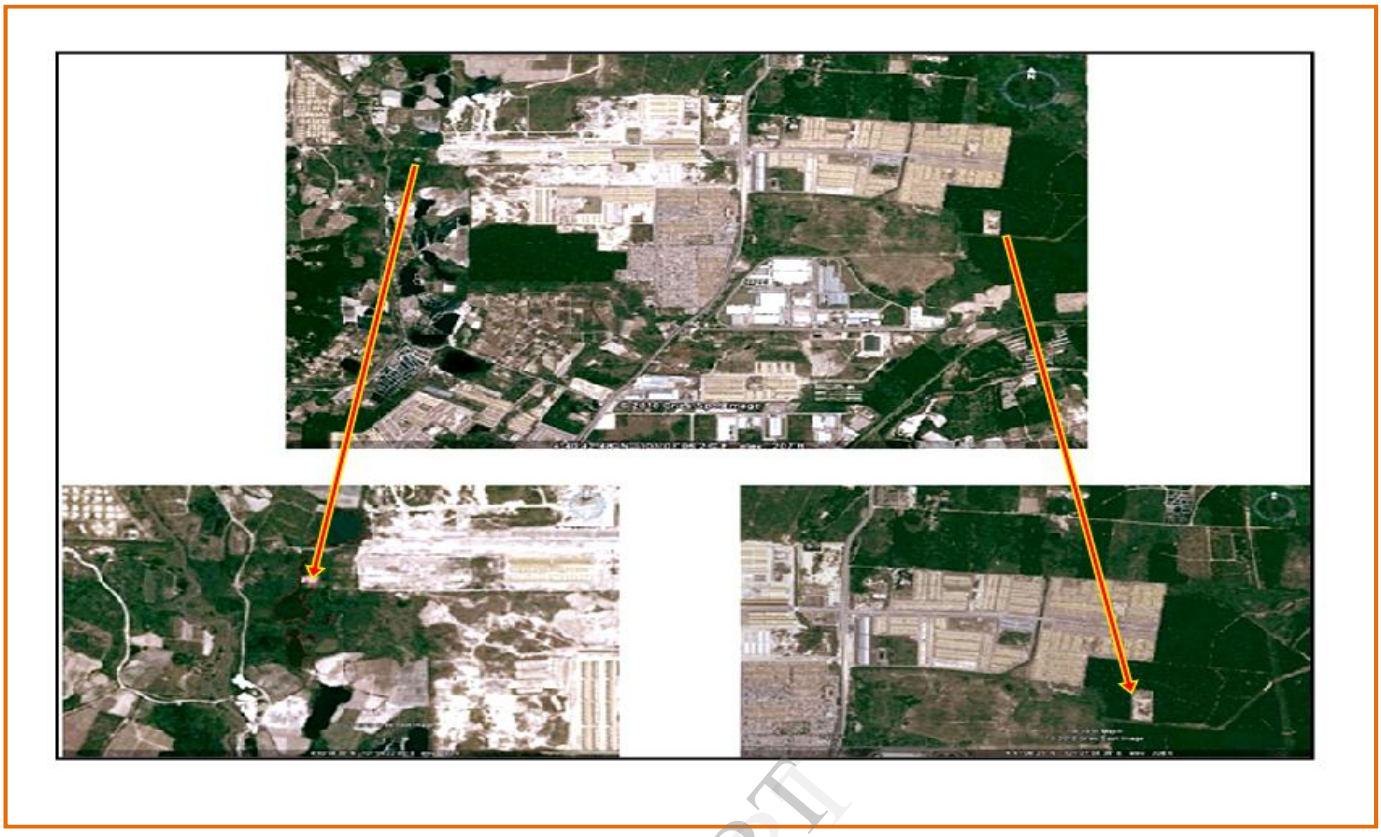

Figure 3: Google earth Satellite spot image (2010) showing the location of construction site #1and site #2 in Klebang Raya north of Ipoh city (Kinta valley)

Old aerial photographs are usually very helpful for the recognition of sinkholes that are now enclosed by buildings or human structures. The thorough elucidation of photographs taken on different dates allows the chronology of freshly formed sinkholes to be inhibited. The interpretations help to gain minimum estimates of the possibility of sinkhole occurrence and permit the study of the spatial-temporal allocated patterns of the subsidence phenomena. Using of low sun-angle photographs with apparent shadows can emphasize subtle topographic features.

The further technique is the investigation of airborne and satellite multispectral and thermal images which may be used to distinguish the surface terrain patterns and acquire the variations in moisture, vegetation, colours, heat related to subsidence areas and sinkholes. In this current work, usage of satellite images of Perak in scale 1/5000 of year (2008). In addition Global Position System (GPS) and Geographic Information System (GIS) Technologies have helped examination considerably. The common methods of mapping land utilizing the changes are typically high in cost and low in precision. The remote sensing provides updated information on land by using these methods. Natural events and human meddling can be observed also by using current and archived distantly sensed data.

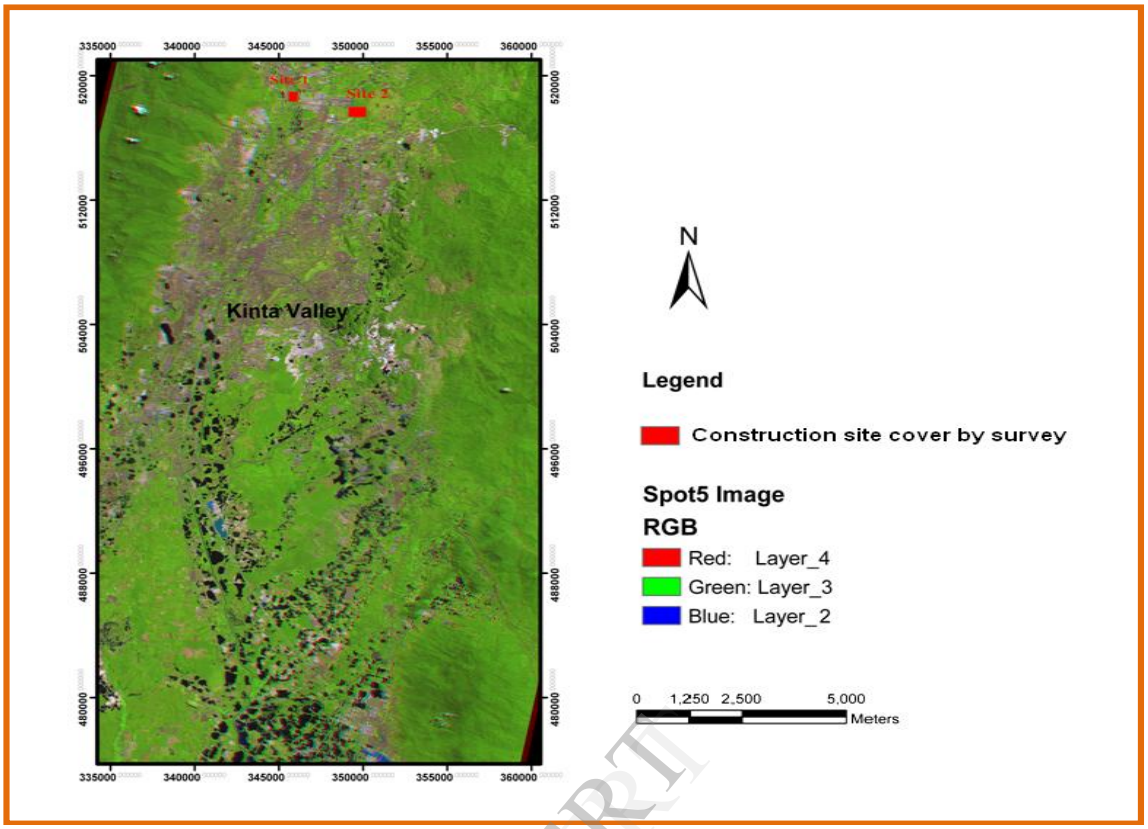

Figure 4: Five layers spot images of Perak state (2008) presenting the location of construction site #1and site #2 north of Ipoh city (Kinta valley)

Interpretation of the aerial photographs of the study area and its surroundings to determine the fracture system, topography and drainage pattern was carried out. These old arial photographs was operational in 1965 under the Colombo Plan have a scale of about 1: 25,000. Table -2 shows the list of aerial photographs used in this study. The technique for this aerial photographic interpretation of the karstic features such as limestone isolated residual hills (mogotes) and the cliffs. Also the lineaments, forests, plantations, etc. The significance of the karstic features and their possible origin in relation to the geologic features are concluding with. Also the interpretation showed that the orientation of lineaments from Main Range and Kledang Range is far from irregular but shows the dominant strike of northwest to Southeast with a subsidiary set striking east-northeast to west-southwest. Conclusion made that these lineaments also observed clearly cutting the marbleized limestone of Kinta valley and the hills above it. An idea about the direction of the lineament in the study area exposed in figure 2, taken from the arial photographs and satellite images and setting on geological map. The drainage in this study area is rather straight and angular and aerial photographs show that stream courses are controlled by the by the direction of lineaments (joints, fractures and fault systems) in the marbleized

bedrock. In addition the arial photographs shown that the area of construction site #1 was swamp area and bushes. The arial photographs shown that the area of construction site #2 was covered with forest and some with oil palm plantation. Furthermore the satellite images' shown that part of forest in site #1 removed for construction project. Furthermore isolated residual limestone hills determine distributed in the south and south west of construction site #2.

Location	Roll no.	Line no.	Print no.
Ipoh	C-12-A	L32N	20-30
	C-6	L31N	20-55
	C-5	L30S	80-90
	C-5	L29N	120-125

Table1: Presenting the list of aerial photographs which employed in this study

Reconnaissance Field Surveys

Through the direct ground inspections in the two construction sites authorize the finding of sinkholes that are not particular on aerial photographs and satellite images due to many reasons. For example, the area may be enclosed by vegetation, sinkholes definite size or their depth is too small to be detected. The recorded model is used for the explanation of each sinkhole, including a diagram of the sinkhole and its access geometry, the covering features with the district and the coordinates, orientation, dimensions, age, continuation degree, vegetation and symbols of volatility as cracks, scarps or pipes. These features supply information on the activity and the periods of the sinkholes and provide as indicators of the plausible location of future sinkholes in proximity to human structures and other observations. The existence of features like muddy areas or the expansion of vegetation and holes crammed with materials may help detect shallow subsidence depressions. Generally, the application of geophysical surveys is desired to establish whether these irregular characteristics are interrelated to sinkholes or not.

Throughout the ground inspection at site#1, no sinkhole was found. On the other hand aerial photographs of the area imply it to be old swamps which might contain sinkholes in the subsurface. More than four big black spots were recognized in aerial photographs, three of them circular to semi circular in shapes and the others are with an extended shape. But due to human activity and excavating work as ex–

mining area, most of these features were packed with sand and other material and among them three area with deposits of grey swamp clay in circular shape were acknowledged. The clay seems to sink down due to numerous causes which will be explained shortly, figure 6; vewing land Photographs viewing the positions of three big black spots were recognized in aerial photographs, that my include sinkholes under the depositional of gray swampy clay construction site #1

Figure 5: land Photographs viewing several positions that recognized in aerial photographs in construction site #1, which identified as the depositional of gry swamps clay

This area identified and demonstrated as an area that might include a medium to large sinkhole extended in the subsurface along this site of visually uncertain depth. This might point to the presence of clay or water in-filled karstic sinkhole or cavities that could intimidate the probity of this site.

During the ground inspection at site #2, two sinkholes was established, but not recognized in aerial photographs and satellite images, because of being enclosed by adjacent small plants. One of these sinkholes with a diameter of ~7m-10m, water in-filled, of visually undetermined depth, recognized and demonstrated as sinkhole

with a narrow showing throat, positioned in the south west flank of this site. The other sinkhole with a diameter of ~35m- 40m. positioned in the north east side of this site, was in-filled with wet clay and other material of sediments due to karst activity, raised a thought that this sinkhole might be linked in the subsurface to one or more of large tabular conduits or channels and my presence of cavities or voids of undetermined depth. Clay or air in-filled karstic sinkhole or cavities were present that could intimidate the veracity of this site. The south section of this site can observe many soil cover collapse with only some meter width and depth.

Figure 6 : Land Photographs viewing a number of sinkholes that identified as water in-fill, empty and covered with vegetation was determined as small and narrow in construction site #2

Location of study area

Construction site #1

Site #1is situated at Klebang Putra – Klebang Green to the north of Ipoh city (Kinta Valley), positioned just about at latitude N4°41'0.96"-N4°41'26.96", longitude E101º05'55.68"-E101º06'21.6" as appeared in Figure6. It locates to the north of the main series and east of the Kledang series.

Figure 7: Location Map, Satellite images and land photograph viewing the location the study area in construction site #1

Construction site #2

Site #2 is situated at Medan Klebang Restu- Klebang Damai to the north of Ipoh city (Kinta Valley), positioned approximately at latitude N4°40'35.04"-N4°41'0.96", longitude E101º07'52.32"-E101º08'18.24" as appeared in Figure7.It locates to the west of the main series of Cameron Highlands.

Figure 8: Location Map, Satellite images and land photograph viewing the location the study area in construction site #2

Field survey technique

Instrumentation and measurement procedure

The survey was conveyed using SAS1000 resistivity meter which has an inherent microprocessor to select the appropriate four electrodes for each measurement automatically. The two dimensional (2D) - electrical imaging/tomography surveys are typically carried out employing a large number of electrodes, 41 or 61 electrodes along a straight line, coupled to a multi-core cable (Griffiths and Barker 1993), in common at a constant spacing of 5m or 10m between adjoining electrodes. When the succeeding measurements were taken, they were configured in a Wenner array and other survey parameters such as the electrical current used is normally converted into a text file which can be read by a computer program. After reading the control file, the computer program then automatically detects the suitable electrodes for each quantity. A laptop computer was engaged to set the RES2DINV inversion software to develop the resistivity model.

In a distinctive survey, most of the fieldwork is in laying out the cables and electrodes. After doing that, the measurements are taken automatically and stocked in the computer. This resistivity procedure usually gives a better grouping of spatial resolution and depth of study in karst terrain than any other geophysical technique.

Figure 9: viewing the instrument type SAS1000 applied in geophysical survey

Data Collection

Electrical resistivity tomography (ERT) was used in order to image the subsurface. Electrical resistivity data composed along two dimensional (2-D) electrical

resistivity profiles were functional above and in proximity underneath and adjoining to active and non-active sinkholes at two construction sites.

Data Collection in Construction site #1

Six electrical resistivity traverses or profiles, Profie-1 to Profile-6 were controlled over and along the survey area, in site #1. The direction of these profiles in (N90°W) and the level of those lines are shown in the location map illustrated in Figure 10.

Electrical resistivity data accumulated along two dimensional (2-D) electrical resistivity profiles, using a 41-channel array in Wenner configuration. The length of each profile was 200.0 m., with an electrode spacing of 5.0m. The space intervals were on average 25.0m between each profile The total length of all profiles in this site was 1200m and cover an area of 30000m^2 , 190 data points were composed for each (41-electrode) in one profile, and on average about 1140 data were composed for total six profiles in this site.

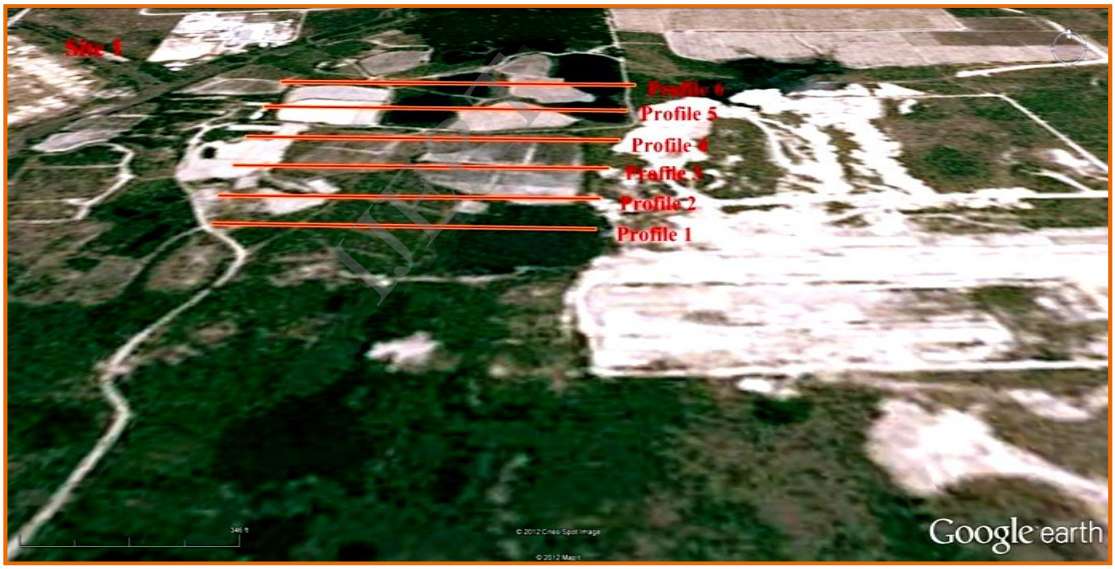

Figure 10: Google earth satellite images viewing the location of resistivity profiles in construction site #1

Data Collection in Construction site #2

Six electrical resistivity traverses or profiles, Profile -1toProfile -6 were conducted over and along the survey area in site#2. The directions of these profiles in (N80º W) and the point of those lines are shown in the location map Figure 11.

Electrical resistivity data were acquired and accumulated to map this site along two dimensional (2-D) electrical resistivity profiles in excess of or beneath to sinkhole, using a 61-channel array in Wenner design. The measurement lengthwise of each

profile was 300.0 m. with an electrode spacing of 5.0m. The space intervals were on average 25.0m between each profile. The total length of all profiles in this site was 1800m, with a cover area of 60000m^2, 320 data points were composed for each (61-electrode) in one profile. On average about 1920 data were collected for total six profiles in this site.

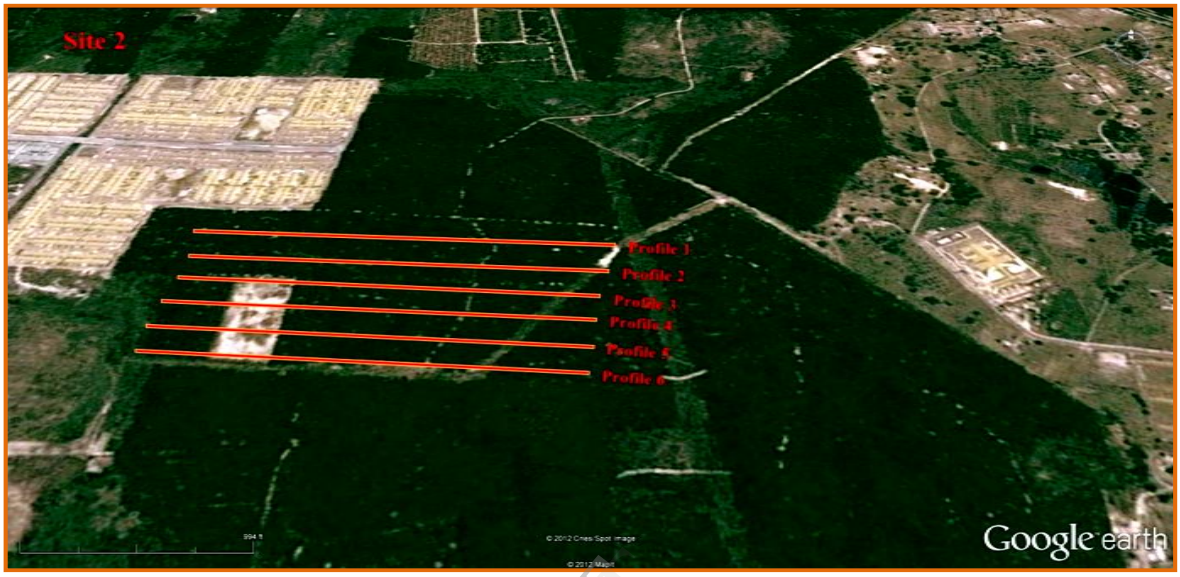

Figure 11: Google earth satellite images showing the location of resistivity profiles in construction site #2

Data processing

After completing the field survey, the resistance measurements are regularly converted to the apparent resistivity values. The data were developed to produce two - dimensional resistivity models of the subsurface. This step is related to convert the apparent resistivity values into a resistivity model section that can be used for geological explanation. The data are readily obtained in the RES2DINV formats the conversion program was outfitted with system. The Root Mean Square (RMS) error statistics enumerate the distribution of the percentage differentiation between the logarithms of the calculated resistivity values and those calculated from the true resistivity model (calculated apparent resistivity values). Data points with errors of more than 30 % percent and above usually are detached. In this survey a small RMS value indicates was less than 10% as defined by the convergence limit. The average default RMS error value in construction site#1 is 4.6 % .The change in the RMS error between iterations with a minimum of 4.0% and a maximum of 15.4%. The average default RMS error value in construction site#2 is 2.58 % .The change in the RMS error between iterations with a minimum of 5.0% and a maximum of 12.6%.

To get a good model, the data must be of uniformly good quality. Bad data points fall into two broad categories or groups:

Systematic noise is reasonably easy to detect in a data set as it is typically present in limited number of readings, and the bad values frequently stick out, easily detached manually from the data set.

It's usually caused by some nature of collapse during the survey such that, the reading does not represent a true resistivity amount. This may due to many causes such as a break in the cable, very poor ground contact at an electrode so that inadequate current injected into the earth or forgetting to attach the clip to one of the electrodes and connecting the cables in the wrong way.

Haphazard noise, include things such telluric currents that affects all the readings and the noise can cause the readings to be lower or higher than the corresponding noise-free readings. This noise is typically more familiar with arrays caused by the large distance linking the two potential electrodes P1electrode and electrode P2. This array tends to single out a large amount of telluric noise. When the noise is of a more arbitrary nature, the noisy data points are not as comprehensible, so it might not be functional to eliminate them manually. Also, manually selection of the bad data points becomes impracticable if there are a large number of bad data points. In some cases, it is not feasible to display the data as simulated sections or profiles. As a common rule, before moving out the inversion of a data set, first take a glance at the data as a pseudo section plot as well as a profile plot. Additionally in these fieldworks all the profiles that contain bad readings for the reason mentions above are redone.

Interpretation resistivity profiles

ERT technique was applied in this geo-electrical survey for the function of investigating sub surface karst features such as sinkholes, due to its relative effort lessens and time correctness. It's founded on the application of electric current into analyzed bedrock and measuring the intensity of electric resistivity to its conduit. Fundamentally, it gives information of electric resistivity resources through the investigated material towards electrical current passageway.

Booming imaging of the bedrocks and features in subsurface karsts terrain is appropriately suitable to make geological classification founded on the variations in electrical resistivity values of the study area into surface of the soil, clay, weathered rock, intact rock, and air-filled cavities. Clays, are usually distinguished by low apparent resistivity's and variables which are depend on moisture, mineral content, purity, and unit shape/size, usually from 5 ohm-m. to less than 60 ohm-m. Sand is usually typified by low apparent resistivity and variables, depending on moisture content, purity and unit size, usually from 70 ohm-m to less than 160 ohm-m. Comparatively weathered limestone rock is typified by high apparent resistivity's typically more than 200 ohm-m to less than 400 ohm-m. Solid or unbroken limestone rock is distinguished by higher apparent resistivities naturally more than 400 ohm-m to more than 4000 ohm-m, and varies depending on layer thickness,

its impurities and moisture content. Air-filled cavities or voids are generally characterized by very high apparent resistivity's, classically >3000 ohm-m - 6000 ohm-m, but varies depending on the conductivity of the nearby strata and size/shape of void or cavity. Dolomitic limestone or dolomite with higher apparent resistivities naturally more than 6000 ohm-m - 80000 ohm-m, and varies depending on layer thickness.

This will be the work charge for electrical investigations survey in these sites to understand the resistivity profiles. Hence, electrical resistivity values were resolute for each rock unit. The results are tabulated in Table 2.

In the following analysis, key explanatory interpretations were prepared to the geophysical electrical data in the selected study areas.

No.	Range of resistivity values	Expected geological units deposits	Color of Res. units in ERT model
1.	0 Ω-m – 5 Ω-m	Insufficient low resistivity, Soft clay with water filled porosity, very high mineralized.	
2.	5 Ω-m – 10 Ω-m	Extremely low resistivity and very high conductivity, soft clay with ponded water, highly mineralized.	
3.	10 Ω-m – 20 Ω-m	Very low resistivity and very high conductivity, Clay moderate mineralized.	
4.	20 Ω-m – 50 Ω-m	Clay low mineralized, low resistivity and very high conductivity.	
5.	50 Ω-m – 70 Ω-m	Below average resistivity, soil, silty or sandy clay.	
6.	70 Ω-m – 100 Ω-m	Average resistivity, clayey or silty sand.	
7.	100 Ω-m – 160 Ω-m	Above average resistivity, sand friable, coarse grain.	
8.	160 Ω-m – 200 Ω-m	Mostly high resistivity, transitional zone consists of rock fragments and sand.	
9.	>200 Ω-m – 400 Ω-m	high resistivity, weathered limestone, probably consisting of wet joints or fractures and/or clay in-fill, higher resistivity	
10.	>400 Ω-m – >3000 Ω-m	Very high resistivity, Compact or intact limestone.	
11.	>3000 Ω-m – 6000 Ω-m	Extremely high resistivity, Voids or cavity, air in-fill.	
12.	>4000 Ω-m – 8000 Ω-m	Extraordinarily high resistivity, Intact pure marbleized limestone or dolostone rocks.	

Table 2: Describes the range of resistivity values with the expected geological unit's deposit

The interpretation of resistivity profiles in Construction site #1

The electrical resistivity data accumulated in this construction site was clarified in

the deficiency of borehole control, by applying table 1above.The interpretation confirms that a massive sinkhole presented in this site and unmitigated between resistivity Profile #1and Profile #6.

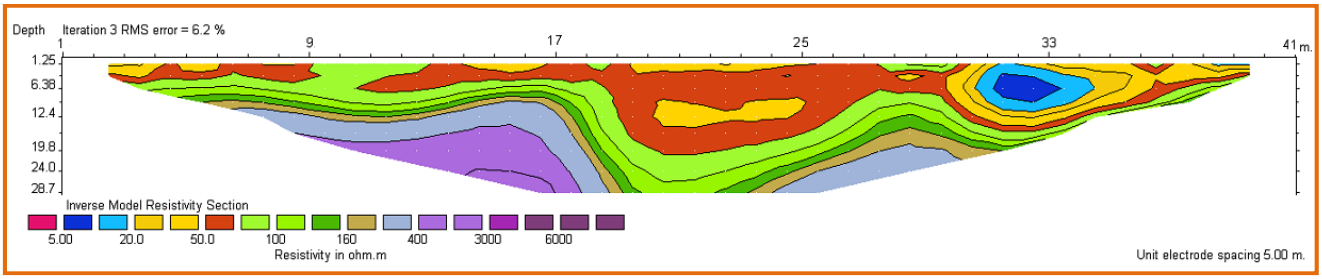

(Figure - A) Inverse model of electrical resistivity section for profiles#1

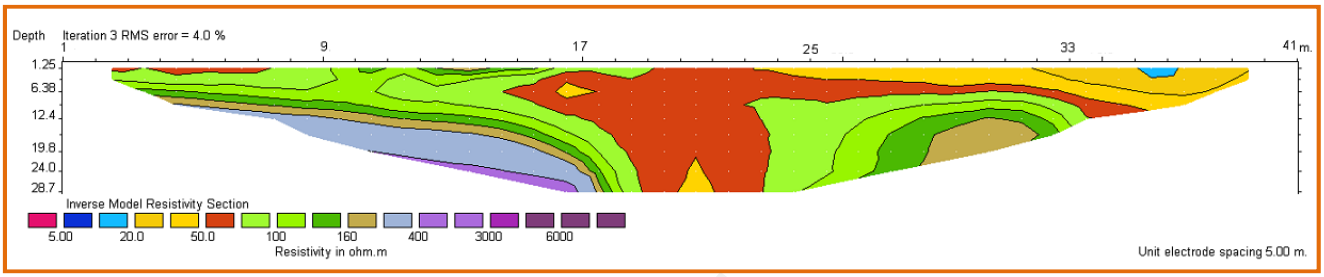

(Figure - B) Inverse model of electrical resistivity section for profiles#2

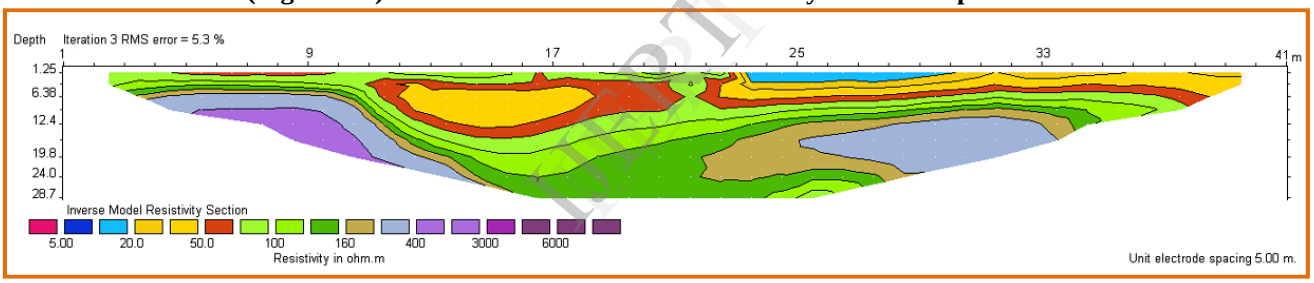

(Figure - C) Inverse model of electrical resistivity section for profiles#3

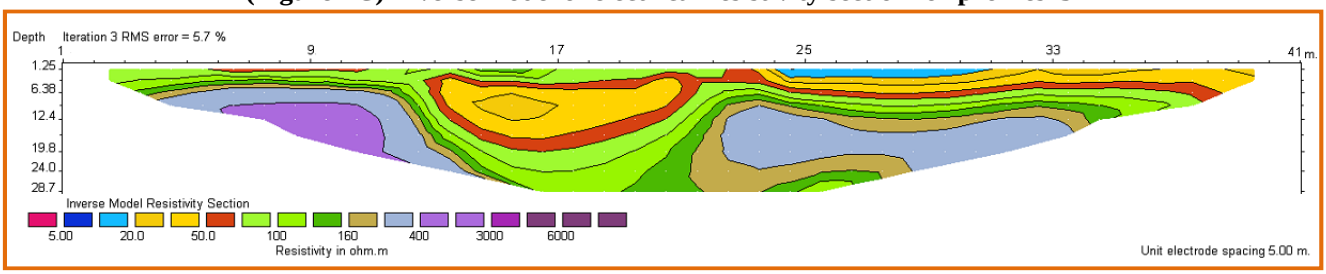

(Figure - D) Inverse model of electrical resistivity section for profiles#4

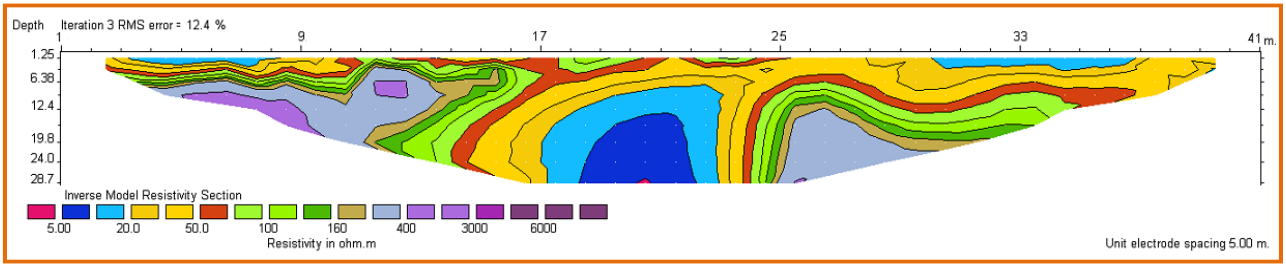

(Figure - E) Inverse model of electrical resistivity section for profiles#5

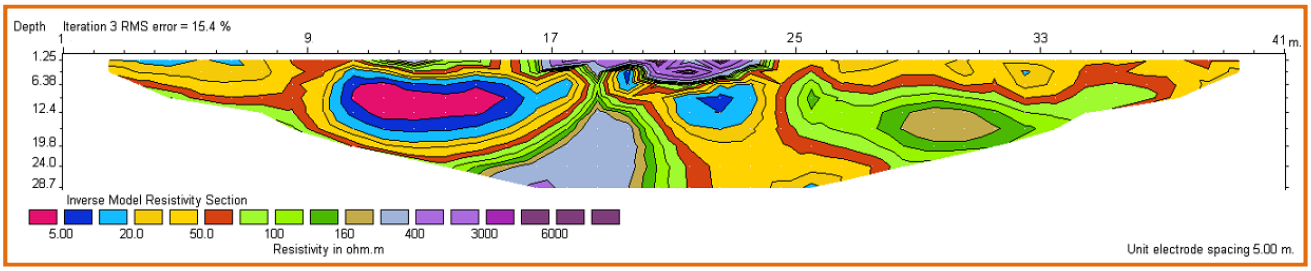

(Figure - F) Inverse model of electrical resistivity section for profiles#6

Figure 12: Inverse model of electrical resistivity section form profiles#1 to profiles#6, viewing the interpreted location of karst features (cavities and sinkholes) in Construction site #1

In resistivity Profile #1, the sinkhole appeared in the core between electrode 17 and electrode 28 with an unbalanced centre between electrode 21 and 22.It stretched in resistivity Profile #2 with these same aspects. In resistivity Profile #4 the position of this sinkhole differentiates, to be forming between electrode 11 and electrode 24, with an uneven centre between electrodes 19 and 20. In resistivity Profile #6 the position of this sinkhole varies also come into view between electrode 18 and electrode 28 with an uneven centre between electrode 21 and electrode 22.The depth of this sinkhole varies, in resistivity profile #1 commencing from the shallowest subsurface depth of <3.0m and continues down to a depth of >28.7m, the bottom being unnoticeable with same aspect as in resistivity profiles #2,#3, #4,#5 and#6.

This sinkhole comprises of sediments with several categories of resistivity values with wide difference, ranging between<5Ω-m and 200 Ω-m. In resistivity profiles #1and #2, the range differs between20 Ω-m -200Ω-m. In resistivity profiles #3 and #4the range differs between 50 Ω-m -200Ω-m.Forresistivity profiles #5 and #6 variation in the range lies between <5Ω-m -200 Ω-m.

The ideal representation of sediments section placed in this sinkhole was originated in resistivity profile#5, with resistivity values in the range between 5Ω-m. -200 Ω-m. Section appears from the upper subsurface to downwards are as follows:

Top deposits, low mineralized clay with low resistivity.
From then on, sandy or silty clay with average resistivity.
Subsequently, silty sand with average resistivity.
Afterward, sand with above average resistivity.
Beneath this, transitional zone consisting of limestone rock fragments and sand with high resistivites.
In the middle of this sinkhole several categories of resistivity values appear as follows:

Soft clay with ponged water, highly mineralized, extremely low resistivity's and very high electrical conductivity opening in the middle of sinkholes from a depth of 14.0m.to attain a depth of >28.0m.
Moderate mineralized clay with very low resistivity's and elevated electrical conductivity adjacent the upper irregularity from a depth of 6.38m.to reach a depth of >28.0m.

This suggests that the beginning of this sinkhole might be from pre-existing fractures which probably widened due to subsidence movement in the area, creating the top layers to crumple down to the limestone bedrock. This then swiftly filled with clay and other materials because of the activity of run-off water on the face.

In resistivity profile #1 patterns of lower resistivity representing oval – shaped lens experimental between electrode 30 to electrode 36 in the shallowest subsurface from a depth of <2.0m ,on-going to a depth of ~ 12.4m. This lens contains deposits with resistivity's values in the series of 5Ω-m -50Ω-m.

Ambiguity with patterns of lower resistivity representing tubular – shaped lens was recognized in resistivity profile #3, at the subsurface directly to the right flank between electrode 22and electrode 39 ,and from a depth of ~1.25 m enduring down to a depth of <6.38m. This tubular – shaped lens bears several types of resistivity values in the range of 10 Ω-m -70 Ω-m. This abnormality mostly consisted of organic gray clay which deposits from the old swamp, which partially extended into resistivity profile #2 and reasonably in resistivity profile #4andprofile #5.

A supplementary anomaly similar to that described above was noticed in tubular – shaped lens in resistivity Profile #5, containing several categories of resistivity values in the range of 10 Ω-m - 70 Ω-m, at the shallowest subsurface directly at the left flank between electrode 3 and electrode 8, commencing from a depth of ~1.25m and continues down to a depth of <3.0m.

Most of the sediments which deposits in resistivity profile #6 form oval - shaped lenses consisting of diverse patterns of resistivity values. One of which was showed in the subsurface directly at the left flank between electrode 10 and electrode 17 from a depth of 1.25m down to a depth of 22m, also containing several categories of resistivity values in the range of>5Ω-m - 50Ω-m,andappeared from the core extending outwards as follows:

Vastly mineralized soft clay with ponded water, extremely low resistivites representing the core of the lens.

Moderately mineralized clay with very low resistivites adjoining the core.
Low mineralized clay with low resistivites in the external most layers of the lens.

The higher most of the subsurface layer in resistivity profile #6were of higher resistivites representing boulders of weathered limestone, and/or fragment of limestone or other rocks, gravel amalgamated with friable sand, emerge between electrode 11and 14,then between electrode 17and 24, from a depth of 1.25 m deep to a depth of ~ 7.0 m

A cavity appeared in the sand at right flank of resistivity profile #6between electrode 25 and electrode 34, from a depth of ~ 11.0m to~15.0m, typically filled with remaining sediment and rock fragments. Limestone bedrock of sturdily widened jointed possibly consisting of wet fractured and/or water or clay in-fill, underneath and adjoining to the sinkhole are clearly seen along these resistivity profile; Figure (12-A, B, C, D, E, F).The surface of this bed was irregular and contains topography with uplifting and hollow space or pits. This unit indicates the remaining unique limestone formation appeared after a procedure of dissolving in subsurface karsts. The intensity of this bed varies between~6.5m - ~12.0 m in left flanks and tumbling down in the middle of these profiles to get a depth of> 28.8 m, reappearing at the right flank at a depth of ~9.0 - ~19.0m.Uninterrupted bedrock of undamaged or un-weathered limestone of very high resistivity's was found in this site, beneath and adjoining to the jointed limestone observed in the left flank at a depth of ~8.0 m - ~15.0 m continuing deep to reach a depth of>28.0 m in the centres of these profiles. It reappears at the right flank at a depth of ~24.0m - ~26.0m Quite a few pinnacles were observed in the subsurface of this site between a depth of ~6.0 m - ~19.0 m; Figure 12- (A, B, C, D, E, F).Table 3 reviewing the intensity of weathered, un-weathered or intact limestone bed rock and the depth of Pinnacles in construction site#1.

The interpretation of resistivity profiles in Construction site #2

The electrical resistivity data gathered in this construction site was calculated in the dearth of borehole control, by applying table 1 above. The interpretation confirms that one longitudinal tubular in consistency was observed in this site and extended between resistivity Profile #1and Profile #3.

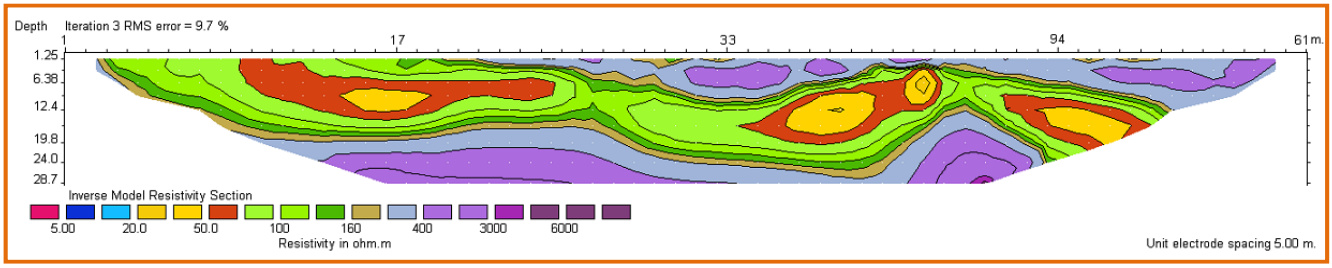

(Figure - A) Inverse model of electrical resistivity section for profiles#1

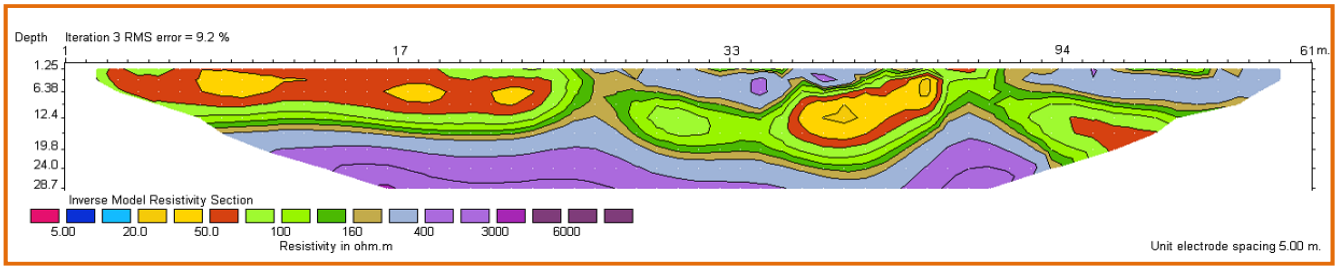

(Figure - B) Inverse model of electrical resistivity section for profiles#2

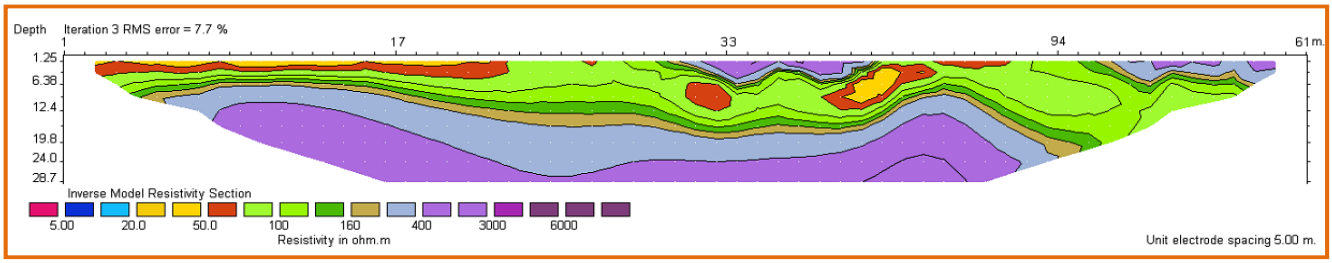

(Figure - C) Inverse model of electrical resistivity section for profiles#3

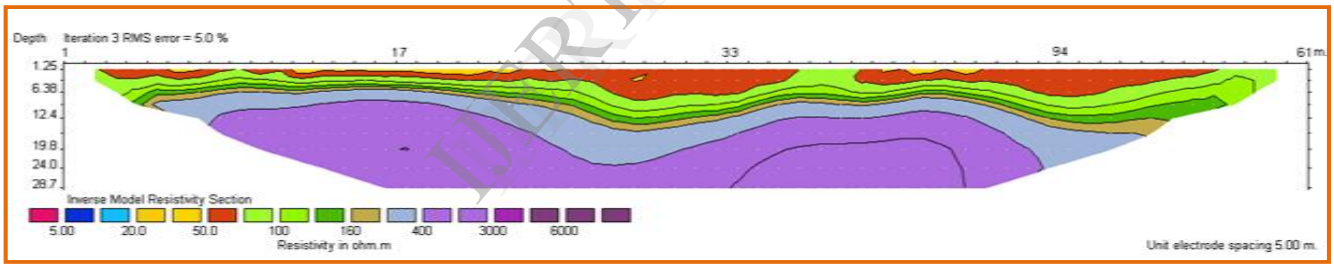

(Figure - D) Inverse model of electrical resistivity section for profiles#4

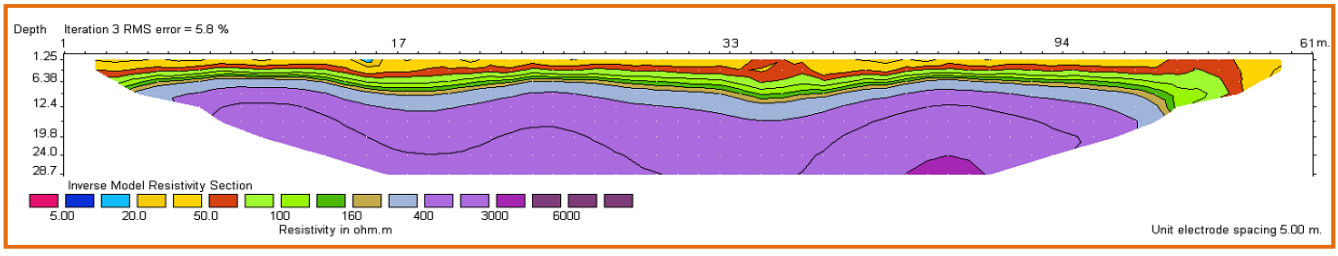

(Figure - E) Inverse model of electrical resistivity section for profiles#5

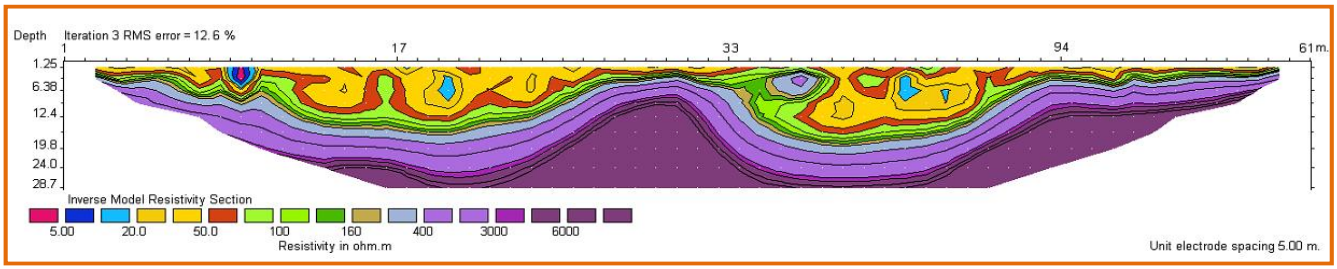

(Figure - F) Inverse model of electrical resistivity section for profiles#6

Figure 13: Inverse model of electrical resistivity section form profiles#1 to profiles#6, viewing the interpreted location of karst features (cavities and sinkholes) in Construction site #2

This site is normally over a high topography area or flat terrain of limestone rocks. The top of the subsurface is categorized by high resistivity, interpreted as a zone of near surface weathered limestone and/or highly jointed limestone with boulders of solid limestone and rock fragments. This zone with an irregular surface magnitudes along three profiles, from profiles#1 to profiles#3 , starting close to the middle of these profiles closely beneath electrode21 to electrode 59 with a depth of ~1.25m to~6.38m ,plunging down to reach a depth of ~9.0m - ~12.0m and rising up to appear a depth of~6.36m - ~12.4 m in the right flank; Figure (13- A- B- C).

Sinkholes were noticed near the surface in resistivity profile #2, commenced in the shallowest subsurface between electrode 40 and electrode 51in right flank, from a depth of <1.25m, sustained deep to reach a depth of ~24.0m. It appeared as a slim to medium wide throat extending about 40m. in diameters. The centre of sinkhole appeared in this profile and expanded inprofile#1 andprofile#3. This sinkhole was linked to one or more larger longitudinal irregularities along these profiles. Tubular cavities of visually undetermined depth emerged as oval-shaped lenses merging together into one tubular channel; Figure (13-A, B, C).

The abnormality detected in resistivity profile #1,profile#2 and profile #3commenced approximately from electrode 3 to electrode 55,in the shallowest subsurface from a depth of <1.25m and sustained deep into the right flank to reach a depth of ~24.0m. It consisted of deposits with several categories of resistivity values in the range of 20 Ω-m to 200 Ω-m and extends outwards from internal to external as follows:

Low mineralized clay with low resistivity and high conductivity coming out as lenses in this tubular incongruity.
Sandy or silty clay with below standard resistivity surrounding the deposits before.
Silty sand with standard resistivity representing the key deposits.
Sand with above standard resistivity.
Rock part of limestone and sand with high resistivities.

This implies that the base of all these cavities were from a pre-existing feature of joints in the limestone bedrock which probably created into prominent solution-widened joints due to the activity of heavy rain and running water on the face which then rapidly packed with clay and other materials.

Region of weathered limestone or highly jointed limestone bedrocks extending across these three profiles was seen beneath and closest to this longitudinal tubular irregularity, with an overall rough surface and categorized with higher resistivity. It is happening in the subsurface at a depth of 6.36m -~9.0m and moved down to reach a depth of ~12.0m - ~17.0m in the centre of this profile, then dropped down to reach a depth of~17.0m -26m. After that it again plunged up to reach a depth of~7.0m.-12.0min the right flank; Figure (13-A, B, C).

Undamaged or non-weathered limestone bedrocks with very high resistivity were found in the subsurface at a depth of ~19.8m along the left flank, in profile #1, profile#2 andprofile#3. It tumbled down to achieve a depth of >27.0m, in the core and continued to the right flank, arise up in a crest shape to reach a depth of ~12.4m.Figure; (13-A, B, C).

Numerous pinnacles of limestone were observed in the subsurface in profile #1, profile #2 andprofile#3. Which were at a depth of ~11.5 m - ~12.4 m, Figure; (13-A, B, C).

In Resistivity Profile#4 and Profile #5, the subsurface karst deposits expand from electrode 3 to electrode 58.The utmost depth of these deposits between ~11.5m -~13.0m in the centre of this profile and a depth of ~13.5m in the right flank Figure (13-E). A number of categories of resistivity values in the range of 20Ω-m to 200 Ω-m emerged with this deposits.

Limestone bed rock with karstification phenomena was visibly observed in the subsurface in both flanks with twin centre appearing beneath electrode 29and electrode49in resistivity Profile#4.It come with a tri-centre in resistivity Profile#5.This irregular zone of weathered limestone expanded across this profile beneath the upper layers, which was overall characterized by higher resistivity. Opening in the subsurface at a depth of ~6.36m to make a maximum depth of ~15.5m. Also in these profiles intact or unweathered limestone bedrock was found at a depth of ~7.5m to ~12.0m in the left flank, plunging down at a depth of ~9.0m.-~22.0m in the centre and at a depth of ~ 17.0m to - 24.0m in the right flank. Several Pinnacles of limestone was discovered in the subsurface beneath these profiles at a depth between ~ 6.0m - ~7.0 m; Figure (13-D, E).

In resistivity profile #6**,** multi-sinkholes were observed. One between electrode 11

and electrode 26 with maximum depth of ~15.5m beneath electrode 19 and the other between electrode 36 and electrode 47with maximum depth of ~18 m beneath electrode 39 . In addition, deposits with numerous categories of resistivity values crammed with these sinkholes, ranging from 20Ω-m to 200 Ω -m. Lenses of lower resistivity values from 10Ω-m to 20 Ω -m. were found. In addition, immature cavity was located in the sand between electrodes 35 and electrode 37,at a depth of ~1.25m , down to a depth of ~8.0m ,of ~10m width and ~6.75m height, with enormously high resistivity typically air-infill.

Immediately under electrode 9 till electrode 10, from the surface down to a depth of ~8.0m., a minute sinkhole was located, containing several categories of resistivity values ranging from 5Ω-m to 20Ω -m. The middle of this sinkhole consists typically of soft clay with ponded water. Reasonably mineralized clay was found adjacent to the preceding deposit. The existence of clay filled karstic cavities or sinkholes which observed in this site could intimidate the reliability of this site because the clay could fall down when subjected to piping under load.

The limestone bedrock visibly observed in the subsurface along this profiles hold very high resistivity with the development of karstification phenomena, which described rough carbonate bedrock containing many peaks and troughs, started with a zone of weathered limestone and/or highly widened jointed limestone bedrock expanding across this profile overlooked beneath the upper layers at a depth of ~3.5m. down to reach a maximum depth of ~18.0m.that was overall characterized with higher resistivity. This was maintained by intact or un-weathered limestone bedrock with very high resistivity, observed in the subsurface at a depth of ~4.0m in both flanks, tumbling down to reach a maximum depth of ~22.0m in the centre.

Limestone pinnacles were noticeably observed at the subsurface in middle of this resistivity profile, between depths of ~3.5m to- ~4.0m (Figure13-F). Table 4 presenting the depths of weathered, un-weathered or integral limestone bedrocks and pinnacles in construction site#2.

Depth of limestone bed rock in the construction site#1 and#2:

Nearby karst terrains normally cause difficult ground conditions to engineers. It's often inefficiently understood by engineers apart from those who are familiar with soluble rock. For engineers, limestone creates various difficulties that enhance in scale and difficulty with increased expansion of the karsts morphology.

The two tables below present an outline or portrayal of some selected points regarding the limestone bed rock depth of the two construction sites that will be favourable for engineers to recognize the depth of limestone in the two

sites under study. These are, however, incomplete and can give only common suggestions of projected ground conditions even though there may arise enormous discrepancy of the depth in the local feature.

No.	Construction site #1	Approximate depth of weathered limestone	Electrode No	Approximate depth of intact limestone bedrock	Electrode No	Approximate depth of pinnacle	Electrode No
1	Res Profile #1	11.0 m 13.0 m 8.0 m 19.8 m >28.0 m 19.0m	7 11 16 18 19 - 24 28	15.0 m 18.0 m 14.0 m	8 11 15	7.0 m 19.0 m	16 28
2	Res Profile #2	10.0 m 12.4 m 24.0 m > 28.0 m	5 9 17 18	19.0 m 24.0 m > 28.0 m	10 16 17	-	-
3	Res Profile #3	6.5 m 18.0 m > 28.0 m 9.0 m	4 12 16 - 25 31	10.0 m 8.5 m > 28.0 m	4 9 14	6.0 m	10
4	Res Profile #4	8.5 m 6.38 m 18.0 m > 28.0 m 9.0 m 12.0 m	4 9 13 15 23 33	8.0 m 19.8 m	6 - 10 12	6.0 m	10
5	Res Profile #5	7.0 m 10.0 m 3.0 m > 24.0 m 12.0 m 22.0 m	4 10 12 15 26 30	8.0 m 10.0 m 18.0 m > 28.0 m > 26.0 m	5 9 10 15 - 24 26	3.0 m 11.0 m	12 26
6	Res Profile #6	26.0 m 12.0 m > 28.0 m	15 19 20	26.0 m	16 - 17	12.0 m	19

Table 3: Reviewing the depth of limestone bed rock in construction site#1

No.	Construction site #2	Approximate depth of weathered limestone	Electrode No	Approximate depth of intact limestone bedrock	Electrode No	Approximate depth of pinnacle	Electrode No
1	Res Profile #1	1.25 m 15.0 m 26.0 m 11.0 m	21 - 59 9 - 26 38 44	23.0 m > 28. 0 m 15.0 m	13 36 44	12.4 m	43
2	Res Profile #2	1.25 - 16.0 m 1.25 - 9.0 m 15.0 m 12.0 m 26.0 m 12.0 m	27 - 40 47 - 57 9 - 21 26 38 43	19.8 m > 28.0 m 17.0 m	11 - 21 38 44	12.4 m 11.5 m	26 44
3	Res Profile #3	9.0 m 6.38 m 17.0 m 7.0 m	6 12 33 43	19.8 m >27.0 m 12.4 m	8 25 43	6.36 m 9.5 m	11 43
4	Res Profile #4	9.0 m 15.5 m 6.36 m	6 28 43	12.0 m 22.0 m 10.0 m 24.0 m	8 28 43 50	6.0 m 7.0 m	17 43
5	Res Profile #5	8.0 m 10.0 m 10.0 m 6.0 m 14.0m	4 17 33 44 54	7.5 m 9.0 m 8.5 m 17.0 m	10 24 43 54	6.0 m 6.36 m 6.0 m	10 24 44
6	Res Profile #6	3.5 m 18.0 m 3.5 m 18.0 m 3.5 m 3.0 m	3 19 30 39 43 59	4.0 m 18.0 m 4.0 m 22.0 m	3 22 30 39	3.5 m 4.0 m	30 49

Table 4: Reviewing the depth of limestone bed rock in construction site#2

Results and Discussion

This current Electrical Resistivity Tomography (ERT) survey at several divisions of the housing complex structure sites in the north of Ipoh city was conducted to figure the subsurface geologic features including sinkholes, karstic voids or cavities and the subsurface geologic structures together with intensely fractured zones and faults. An assessment of the situation was surmised from the subsurface images. Subsequently an estimation of the possibility of a crumple occurring due to these cavities or voids was prepared.

This study also displayed that high resolution Electrical Resistivity Tomography (ERT) can be effectively implemented to reflect the bedrocks and the fractures in subsurface carbonate karsts terrain. The resistivity method used in this study was

very favourable in locating underground voids or fractured zones. It's also completely suitable for differentiating surficial soil, clay, weathered rocks, compact or intact rocks and air-filled karstic voids or cavities and intensely fractured rocks. These features have an effect on many construction site locations in areas extended over carbonate rocks, causing disturbance in construction works which can supply to the maximization of the overall cost.

The geological model clarified from the geophysical data, consists of a basal limestone unit which comprises the bedrock, enclosed by soil or sandy clay. This bedrock unit that appears to be dissected or intervened by cavities high-flying to solution-widened joints is interpreted as karstic processes. These features are perilous because they are in-filled with thick clay, others with sandy or salty clay that could collapse when subjected to piping under load.

The geophysical data indicated that the depth of limestone bedrock was asymmetrical. In construction site #1, the depth of weathered limestone bedrock mixed between 3.0 m and >28.0m. For integral limestone bedrock, the depth varied between 8.5 m and >28.0m. And the depth of pinnacles varied between 3.0 m. and 12.0m as shown in the table -4. And in construction site #2, the depth of weathered limestone bedrock mottled between 1.25 m and 26.0m. Intact limestone bedrock the depth varied between 4.0 m and >28.0m. And the depth of pinnacles varied between 3.5 m and 12.4m as shown in the table -5.

The geophysical data in construction site #1 indicated an area of lesser resistivity and high conductive ambiguities where the top layers had been lowered by fracture along the site and the resulting sinkhole due to the collapse, thus containing soft clay with vastly mineralization and some ponded water has made the area less resistive to electrical current. This was noticed in the site during the dugout works. The data also exposed that this sinkhole continues to produce in the subsurface at most of this site and was in fact extended in six locations of the six resistivity profiles in this site.

The geophysical data in construction site #2 showed an area of lower resistivity and high conductive ambiguities, which has been affected by sinkhole and many tubular ambiguities thus contain clay and sandy clay. The bedrock unit appears to be analysed by many features like sinkholes, cavities and channels. These features are harmful because they are packed with thick clay, sandy or silty clay that could fall down when subjected to piping under load. The high resistivity ambiguities, indicating the existence of karstic voids are needed to be confirmed by the drilling results.

These analyses led to the conclusion that the beginning of the sinkhole and cavities in construction site #1 was a pre-existing fracture which had widened possibly due to subsiding movement in the area, creating the collapse of top layers down to limestone bedrock which then was crammed with clay rapidly because of the activity of run-off water on the surface. The origin of the sinkholes and cavities in construction site #2 appeared to be a new one. The origins of all these cavities were previously thought to be of pre-existing features like joints in limestone bedrock. It had formed into a strongly outstanding solution-widened joint for the activity of rain

fall and running off the water on the surface then swiftly being packed with clay and other materials.

The sinkholes in the study area were characterized with reference to the mechanisms of the ground malfunction and the nature of the material which fails and subsides. In construction site#1 the sinkhole is a collapse which is the type, created by a small-scale collapse which has provided the surface the subsurface structural features. Then the earliest collapse sinkhole was packed with soil, sediment and fragments due to modify of the surroundings and finally resulting in the sinkhole being buried. Surface subsidence may then take place due to compaction of the soil.

The sinkhole in construction site#2 is a suspension sinkhole by type, created by slow dissolution of the limestone bedrock. They are common features such as joints of a karst terrain that have developed over geological time scales. The larger features still have potentially unsound rock mass somewhere beneath their lowest point. The majority dissolution features are deep holes and pipes. These are produced at isolated stream sinks and swallow holes, where the form looks like conical sinkhole created largely by scattered water percolation.

The geophysical data also indicated that sinkholes were originated in many locations. The most hazardous area was found underneath resistivity profile #6 in construction site #1 with sinkholes extending over 55m, reaching depths of more than 28.7m. Another harmful area was beneath resistivity profile #6 in construction site #2 with two main sinkholes, one of them extending 75.0m.with highest depth of ~15.5m. and the other extending about 55.0m. with maximum depth of ~18.0 m. These features are harmful because some are in-filled with thick clay and others are in-filled with sandy or silty clay that could collapse when subjected to piping under load.

In accordance with to the characteristics of morphological features of karstic ground conditions by (A. C. Waltham and P. G. Fookes, 2005), the karst in construction site site#1 found between profile 1 and profile 6 is an older or complex karst KIV. The karst in construction site#2 found between profile 1 and profile 3 is a youthful karst KII. Afterwards the karst type changed over profile#5 to profile #6 to mature karst KIII.

Once starting the excavating work over the resistivity profile#5 in construction site#1, underground water flow up straightforwardly, this confirms the geophysical survey, that there was a source of ground water body under this profile.

Planning to Mitigate the Risk in Construction Sites Developing over carbonate Karst Terrains

Early planning to diminish the risk of structures in housing complex construction sites over karstified carbonate rock is the most reasonable move towards the improvement of the sites.

Three solution methods most generally used in the plan to diminish risk of the trouble areas in construction site# 1 are:

The first solution: Sinkhole remediation by using reverse grading technique. To filling this huge sinkhole, in the beginning must excavating the hole and then plug the throat by concrete block or can be sealed with thick grout of cement or filling the hole with larger boulders or rocks at the bottom. Follow with cobble, then gravel or bentonite mixed with rock fragments, then sand, and finally at the top must cover with 8-12 inches of soil. The placing of larger material directly on bedrock at the bottom of the sinkhole to providing the support and prevent another collapse to happen. While the smaller material will stops water from moving the soil downward into the void in the bedrock.

The second solution : The other solution drilled piles setting to sound rock strata then filling with geo graded materials to prevent the sinkhole collapse. If the sinkhole or cavity is dangerous to designed foundations, must packed with concrete and using the bridging beam to transferring the load to the side of sinkhole.

The third solution: Relocating the load to sound rock strata because the sinkhole is dangerous to designed foundations, and leave the area for garden, playground or golf course.

Three solution methods most frequently used in the plan to diminish risk of the problem area in construction site# 2, are:

The first solution: Regular shallow spread footings with or without soil development, rigid mats and grade beams, and deep foundations (piles and piers) which must attain the bed rock. Heavy geo grid can be used as well to strengthen the soil over voids and lessen the impact of any future disastrous void collapse. Grouting may also be engaged to fill fractures and small voids in rock head, preventing them to spread.

The second solution: Relocation of footings or of the whole structure, when possible, may be proved to be more cost-effective in some cases.

The third solution: Grouting by the chemical solution forms which injected into the cracks, to seal the joints and fractures. Chemical grouting is well-suited for channels and for stabilizing the soil around the channel for mitigating settlement of overlying structures within the influence of the channel configuration. Grout is injected in drilled holes along the flow paths of the channel, sealing and preventing flow any rain water through them in future.

Hazards can also be prohibited by controlling the irrigation round the both housing complex sites by using water point irrigation method and redirecting surface water overflow by using elastic pipes with telescopic joints to get unnecessary water to water rainfall channel. Also applying a tar coating to this water rainfall channel, water taking out from the land can be barred.

Conclusions

This paper demonstrate the performed of integrated techniques were across two

housing complex construction sites north Ipoh city, Perak state, peninsular Malaysia.

geological, geophysical, aerial photographs and satellite images were used as identification techniques to figure out the subsurface in carbonate karsts terrain because the tool is appropriate for differentiating surficial soil, clay, sand, weathered rock, intact rock and water - air-filled cavities.

Two-dimensional (2-D) electrical resistivity profiles were conducted over two construction sites. Construction site #1 is located at Klebang Putra – Klebang Green and Construction site #2 is located at Medan Klebang Restu-Klebang Damai, north Ipoh city.

ERT technique was used in this geoelectrical survey for the reason of investigating the sinkholes and other karst features due to its less relative effort and time effectiveness. An assessment of the situation was surmised from the subsurface images. Subsequently an estimation of the possibility of a collapse occurring due to sinkhole was prepared. Interpretation of geophysical data indicated that both low resistivity and high conductivity anomalies extend along the proposed area in both construction sites.

Consequently, early planning is required to minimize the risk to structures in these construction sites over karstified carbonate bedrock. Initial consolidation of geo grading technique, driven piles to rock head pinnacles and control the drainage works must be put into operation in these sites.

References

C. Waltham1 and P. G. Fookes, 2005, engineering classification of karst ground conditions, Quarterly Journal of Engineering Geology and Hydrogeology, v. 36, p. 101-118.

Dahlin T., 1996, 2D resistivity surveying for environmental and engineering applications. First Break, v. 14(7), p. 275-283.

Hoover R. A. and Saunders W.R., 2000, Evolving Geophysical Standards, *in* Proceedings, The First International Conference on the Application of Geophysical Methodologies & NDT to Transportation Facilities and Infrastructure Conference Proceedings, Missouri Department of Transportation.

Hussein, I. E., Kraemer, G. and Myers, R., 2000,Geophysical characterization of a proposed street extension in Cape Girardeau, Missouri, *in* Proceedings, The First International Conference on the Application of Geophysical Methodologies & NDT to Transportation Facilities and Infrastructure.

Ioannis F. Louis, Filippos I. Louis and Melanie Bastou, 2002, Accurate Subsurface Characterization For Highway Applications Using Resistivity Inversion Methods, Geophysics & Geothermic Division, Geology Department, University of Athens, Panepistimiopolis,Ilissia, Athens.

Loke, M. H. and Barker, R. D. 1994. Rapid least-squares inversion of apparent resistivity pseudo-sections, Extended Abstracts of Papers 56th EAGE Meeting Vienna, Austria 6-10 June 1994, p. 1002.

Loke, M.H., 1994, The inversion of two-dimensional resistivity data. Unpubl., PhD thesis, University of Birmingham.

Loke, M.H., 1999, Time-lapse resistivity imaging inversion, in Proceedings, 5th Meeting of the Environmental and Engineering Geophysical Society European Section, Em1.

Muhammad, R. F. &Yeap, E. B. 2002, Estimating Dissolution Rates in Kinta and Lenggong Valleys the Micro Erosion Meter, Geol Soc Bull. V. 45, p. 26-27.

Muhammad, R. F, 2003, The Characteristic and Origin of the Tropical Limestone Karst of the Sungai Perak Basin, Malaysia, Unpubl. PhD, University of Malaya, p. 443

Niel A. Yahia, Yassin R. Rafeeq,Samer R. Hujab , 1994, The application of complex geophysical techniques to detecting and locating the Weakness zone and the water seepage in the body of the AL-Tharthar dam , Samara Town, Salahuddin province, Iraq geosurv, Baghdad – Iraq.

Neil L. Anderson, Derek B. Apel and Ahmed Ismail, 2007, Assessment of Karst Activity at Highway Construction Sites Using the Electrical Resistivity Method, Missouri, USA.

Psomiadis David , Tsourlos Panagiotis, Albanakis Konstantinos, 2008,Electrical resistivity tomography mapping of beach rocks, application to the island of Thassos (N. Greece), Environ Earth Sci (2009), v. 59:233–240, DOI 10.1007/s12665-009-0021-9.

Sowers GF, 1996, Building on sinkholes, American Society of Civil Engineers, New York.

Telford, W.M., Geldart, L.P., and Sheriff, R.E., 1990, Applied Geophysics, (2nd add). Cambridge University Press, New York

William E. Doll', Jonathan E. Nyquist2, Philip J. Carpenter3, Ronald D.Kaufmann4, and Bradley J. Car-r', 2002, Geophysical Surveys of a Known Karst Feature, Oak Ridge Y-12 Plant, Oak Ridge, Tennessee

W. Zhou 7 B.F. Beck 7 J.B., 2000, Stephenson Reliability of dipole-dipole electrical resistivity tomography for defining depth to bedrock in covered karst terrains.

Yahia, Nail Abdel Al-Qadir, Yassin, Riyadh Rafeeq, Abdel Al-Qadir, Sabah Omar, 1994, The results of Application of geophysical Techniques in the exploration of Bauxites Ore deposits in subsurface karsts terrains, Iraqi Western Desert, Rep.no2262,geosurv, Baghdad – Iraq.

Yassin, Riyadh Rafeeq, 2002, evaluates the presence of karstic Bauxitic clay deposits in parts of western desert of Iraq by the application of VLF – electromagnetic and Electrical resistivity techniques, Masc. thesis submitted to Department of Geology, college of science, university of Baghdad, p. 293.